04

Radiation amplification by aperiodically unstable plasma formed by multiphoton ionization of inert gas atoms

© K.Yu. Vagin

Lebedev Physical Institute, Russian Academy of Sciences,
119991 Moscow, Russia
e-mail: vagin@sci.lebedev.ru

Received March 17, 2025
Revised August 12, 2025
Accepted October 13, 2025

The interaction of electromagnetic radiation with half-limited nonequilibrium plasma pre-formed by multiphoton ionization of dense inert gas atoms is considered. It is shown that due to the aperiodic electromagnetic instability development in such plasma, it is possible to amplify the fields penetrating into the plasma and reflected from it by several orders of magnitude. For a density of ionized gas close to atmospheric density, the growth rate of the fields strength falls into the terahertz frequency range.

Keywords: photoionized plasma, electromagnetic instabilities, terahertz radiation.

DOI: 10.61011/TP.2026.02.62876.37-25

Introduction

Impact of short electromagnetic laser pulses with various polarizations on gas atoms leads to generation of photoionized plasmas having a set of unusual physical properties, which are essentially different from the properties of equilibrium plasma with near-Maxwellian electron distribution. In addition, both full ionization of gas atoms by high-power pulses in tunneling mode [1–5] and generation of weakly ionized plasma under the action of moderate-intensity laser light in multi-photon ionization mode [6–13] are possible. Depending on certain ionization conditions, there is a wide variety of generated photoelectron distributions both by energies and pulse directions. Non-equilibrium state of particle distributions in photoionized plasma is a common combining property, which may cause evolution of various instabilities in plasma. Evolution of instabilities in turn leads to accumulation of excess electromagnetic field energy in plasma [14], and this energy may be used for radiation amplification and generation, which is one of extremely important present-day tasks of research in various scientific and technology areas, including plasma physics.

Radiation amplification in conditions of tunnel ionization of gas atoms is possible owing to the evolution of plasma instabilities associated with strong anisotropy of the generated distribution of photoionized plasma electrons induced by ionizing radiation polarization. In particular, when gas atoms are ionized by linearly polarized radiation, an electron distribution close to anisotropic bi-Maxwellian distribution is formed [1,2], while in the case of ionization by circularly polarized radiation, a toroidal electron velocity distribution is formed [1,3,4]. Specific features of instable eigen modes and features of electromagnetic radiation amplification in such plasmas, including spatially confined, are discussed in detail, for example, in [15–20]. A much wider variety of non-equilibrium photoelectron distributions and consequently of instable modes is induced by multi-photon ionization of gas atoms [6–10]. In particular, during such ionization of inert gases, highly anisotropic photoelectron distribution is formed initially and then quickly with time becomes isotropic, but multi-peak energy distribution. Papers [21–27] are devoted to the study of potential and electromagnetic instabilities and identification of conditions for radiation amplification in plasma generated via multi-photon ionization of inert gas atoms at different plasma evolution stages. In conditions of ionization of relatively dense gas with near-atmospheric pressure, frequencies of photoelectron collisions with neutral atoms appear to be comparable with electron plasma frequency. Therefore, description of radiation propagation and amplification in such plasma shall include, along with non-equilibrium photoelectron distribution, the aspects of photoelectron scattering by neutral atoms [27]. Note that in the given conditions, the typical process frequencies fall within the THz range. This indicates that the THz radiation amplification mechanism described in this paper can be used, together with a previously proposed (see, for example, [28–30]) opportunities of THz radiation generation via atom ionization in moderate-intensity laser fields.

This work is focused on the action of test electromagnetic radiation on weakly ionized non-equilibrium plasma pregeenrated under the action of intense femtosecond laser pulse in conditions of multi-photon ionization of inert gas atoms. Section 1 uses linear approximation by the test radiation field amplitude for simultaneous closed-form solution of the initial and boundary problems relying on the self-consistent solution of kinetic equation for perturbation of the photoelectron velocity distribution function, and of Maxwell's equations for fields in semiconfined plasma involving the Laplace time transform. Integral expressions

for plasma-reflected wave and plasma-penetrating radiation fields in the case of arbitrary incident wave profile

were derived without explicit breakdown of highly non-equilibrium photoelectron energy distribution. Elastic scattering by neutral atoms, which is the key process for photoelectron dynamics in dense weakly ionized plasma, was described kinetically using the collision integral

similar to that used in the Lorentz model [31]. Special focus in this work was made on consecuitive consideration of the Ramsauer–Townsend effect [32–34] on the frequency of photoelectron collisions with neutral atoms. An abrupt non-monotonic velocity dependence (corresponding to this effect) of the transport cross-section of elastic photoelectron scattering by atoms in a wide energy range relevant for the multi-photon ionization condition may be employed for closed-form calculations using the approach described in [24,27,35] and applicable to particular experimental data for various gases (see, for example, [36,37]. This sets our approach apart from works, which use particular power interpolations [22,38] for simulating the scattering cross-section in comparatively narrow photoelectron energy ranges. Individual features of time evolution of particular non-equilibrium plasma and interaction between the plasma and electromagnetic radiation, primarily, radiation amplification, are defined to a great extent by dispersion properties of instable eigen modes of such plasma [39], which are necessary for the inverse Laplace transform performed when calculating the field time dependence. For the cold photoionized plasma model, whose isotropic non-equilibrium photoelectron distribution is described by a monoenergetic peak without broadening, Section 2 provides an explicit expression for transverse permittivity, which makes it possible to derive dispersion equation for eigen electromagnetic modes of such plasma. In the complex frequency plane across the entire range of possible wavelengths, solution of this equation is described in detail for an instable mode, whose most effective amplitude increase is implemented in the long-wavelength limit and corresponds to aperiodic time rise. Accurate closed-form solution of dispersion equation for the maximum increment of this aperiodic instability is provided. By way of example of Xe gas for two different photoionized plasma cases, parameter values are given and numerical estimates are made for typical non-equilibrium photoelectron distribution lifetimes and instability evolution time. A wide energy range was established for photoelectrons, for which evolution of this aperiodic instability was possible. Section 3 uses the results from the previous sections to explore analytically and numerically the spatiotemporal electromagnetic field structure, which is induced by the instable plasma response to the incident pulse action, in the entire space. It is shown that the effectively amplified part of both plasma-penetrating and plasma-reflected fields rises anharmonically, and the spectral composition of these signals is set by the maximum increment of aperiodic photoionized plasma mode and weakly depends on the test radiation frequency, whose effect significantly defines the plasma response amplitude. Asymptotic closed-form expressions for time-rising fields were derived, and conditions for the most effective amplification of incident radiation on plasma were established.

1. Incidence of electromagnetic pulse on semiconfined photoionized plasma

Consider weakly ionized plasma preliminary formed through multi-photon ionization of monoatomic gas by a short linearly polarized laser established. Non-equilibrium photoelectron distribution formed after deactivation of the ionizing pulse and distribution evolution phases are discussed in detail in [21,23,24]. Under the action of low-intensity pulses $\sim 10^{12}-10^{13}\,\mathrm{W/cm^2}$, atom ionization is implemented through absorption of a minimum amount of photons, which is necessary to overcome the atom ionization potential. Energy spectrum of highly non-equilibrium photoelectron distribution looks like a narrow peak, whose position doesn't exceed several electron-volts [6,7,21]. The degree of ionization of the generated plasma formation is low $\sim 10^{-6}-10^{-4}$ [21]. Therefore, photoelectrons are primarily scattered by neutral atoms, and electron collisions with each other and with ions are rare. For the specified typical energies, photoelectron scattering by atoms is elastic in nature [36,37]. In a relatively dense plasma, frequent photoelectron collisions with neutral atoms characterized by the frequency $\nu(v)$, where v is the electron velocity, lead to fast relaxation along the pulse directions and at times exceeding ν^{-1}, the non-equilibrium photoelectron distribution function becomes isotropic $f_0(v)$. In plasma with a quite low degree of ionization, the above-mentioned non-equilibrium photoelectron velocity distribution is maintained during a sufficiently long time interval until relaxation to the equilibrium Maxwellian function, which is induced either by rare electron-electron collisions or by photoelectron collisions with heavy neutral atoms [40].

Suppose an electromagnetic wave, whose electric field strength is written as... where $\eta(\tau)$ is the Heaviside unit function, $\mathbf{e}_x$ is the unit vector along the $0x$ axis, strikes the above-mentioned homogeneous photoionized plasma occupying the half-space $z > 0$ at time $t = 0$

$$\mathbf{E}_i\,(t - z/c) = \mathbf{e}_x\,E_i\,(t - z/c)\,\eta\,(t - z/c)\,, \quad z < 0. \qquad (1)$$

The field written as (1) penetrates plasma and is partially reflected back. The reflected field satisfying Maxwell's equations in vacuum can be represented as an outgoing transverse wave from plasma $z < 0$ with the electric field $\mathbf{E}_r(t + z/c) = \{E_r(t + z/c), 0, 0\}$ and magnetic field, which has an identical spatiotemporal dependence and is oriented along the $0y$ axis. Field (1), penetrating into plasma $z > 0$, in turn induces a change in the initial photoelectron distribution function and the electric field $\mathbf{E}(z, t) = \{E(z, t), 0, 0\}$ and magnetic field oriented along $0y$. Being interested in the non-equilibrium plasma response

to the action of external electromagnetic field (1), contribution to perturbations of the photoelectron distribution and electromagnetic field in plasma associated with small thermal fluctuations will be neglected. Then, at the initial time $t = 0$ corresponding to arrival of the incident wave edge at the plasma boundary, there are no perturbations of the given quantities $\delta f(\mathbf{v}, z, t = 0) = 0$ and $E(z, t = 0) = 0$.

In such conditions, to describe the evolution of the electromagnetic field in plasma and of the reflected wave at $t > 0$, we use the Laplace transform, when the original function $\Phi(t)$ and image function $\Phi(\omega)$ are connected by the following relations

$$\Phi(\omega) = \int_0^{+\infty} dt\, \mathrm{e}^{\mathrm{i}\omega t}\Phi(t),$$

$$\Phi(t) = \int_{-\infty+\mathrm{i}\Delta}^{+\infty+\mathrm{i}\Delta} \frac{d\omega}{2\pi}\, \mathrm{e}^{-\mathrm{i}\omega t}\Phi(\omega), \quad \Delta > \gamma > 0,$$

and γ is the exponential factor of $\Phi(t)$.

We are interested in relatively high-frequency collective photoelectron motions, when the motion of neutral atoms and ions may be neglected. Typical photoelectron energies are of the order of an electron-volt, therefore the typical photoelectron velocity is relatively low. Electromagnetic field amplification attributed to instable long-wavelength modes of non-equilibrium plasma is discussed below. Therefore, we can limit ourselves to conditions where the distance $v/|\omega|$ covered by an electron during the field variation time is much smaller than the spatial scale of field variation. The action of the external field is assumed to be relatively weak, thus, the problem of field interaction (1) with non-equilibrium plasma can be solved in linear approximation by field amplitude. Then, for small perturbation of the Laplace image of electron distribution function $\delta f(\mathbf{v}, z, \omega)$, we have a linearized kinetic equation [27]:

$$-\mathrm{i}\omega\delta f(\mathbf{v}, z, \omega) + \frac{e}{m}\frac{\mathbf{v}\mathbf{E}(z, \omega)}{v}\frac{\partial f_0(v)}{\partial v} = -\nu(v)\left[\delta f(\mathbf{v}, z, \omega) - \langle \delta f(\mathbf{v}, z, \omega)\rangle_{\mathbf{v}}\right], \quad (2)$$

where $\mathbf{E}(z, \omega)$ is the Laplace image of the electric field in plasma, e and m are the electron charge and mass. In (2), $\langle \ldots \rangle_{\mathbf{v}} \equiv \int(\ldots)\,\mathrm{d}O_{\mathbf{v}}/4\pi$ means averaging over the velocity vector angles $\mathbf{v}$. Collision integral in (2) describes elastic photoelectron collisions with neutral atoms leading to a change in the electron pulse direction without changing the electron energy [31]. Neglect of a term with a spatial derivative in equation (2) justified in the long-wavelength limit precludes from accurate description of electromagnetic field behavior in plasma on small scales. However, such scales are essential only near the edge of plasma-penetrating radiation where amplification cannot be implemented yet.

Using the solution to kinetic equation (2) for calculation of electric current perturbation in plasma on the basis of self-consistent treatment of Maxwell's equations, we get the following equation for the electric field in plasma:

$$\frac{\partial^2 E(z, \omega)}{\partial z^2} + \frac{\omega^2}{c^2}\varepsilon_{tr}(\omega)E(z, \omega) = 0, \quad (3)$$

where

$$\varepsilon_{tr}(\omega) = 1 + \frac{4\pi}{3}\frac{\omega_L^2}{n\omega}\int_0^{+\infty} \frac{v^3 dv}{\omega + \mathrm{i}\nu(v)}\frac{\partial f_0(v)}{\partial v} \quad (4)$$

— is the transverse permittivity of photoionized plasma calculated without considering the spatial dispersion (which is justified for long-wavelength perturbations), c is the speed of light, $\omega_L = \sqrt{4\pi e^2 n/m}$ is the electron Langmuir frequency , n is the electron density.

Equation (3) shall be supplemented by conditions of continuity of tangential field components in vacuum $\mathrm{e}^{\mathrm{i}\omega z/c}\mathbf{E}_i(\omega) + \mathrm{e}^{-\mathrm{i}\omega z/c}\mathbf{E}_r(\omega)$ and in plasma $\mathbf{E}(z, \omega)$, and their derivatives with respect to z with $z = 0$. Here, $E_{i(r)}(\omega) = \int_0^{+\infty} dt\, \mathrm{e}^{\mathrm{i}\omega t}E_{i(r)}(t)$ are Laplace images of the incident (reflected) electric fields at the plasma boundary with $z = 0$. By solving homogeneous differential equation (3) taking into account these boundary conditions and performing the inverse Laplace transform, we get the following expression for the plasma-reflected field:

$$E_r\left(t + \frac{z}{c}\right) = -E_i\left(t + \frac{z}{c}\right) + \int_{-\infty+\mathrm{i}\Delta}^{+\infty+\mathrm{i}\Delta} \frac{d\omega}{\pi}\frac{\omega}{\omega + \mathrm{i}k(\omega)c}E_i(\omega)\mathrm{e}^{-\mathrm{i}\omega\left(t+\frac{z}{c}\right)}, \; z < 0. \quad (5)$$

Expression for the plasma-penetrating field is in turn written as

$$E(z, t) = \int_{-\infty+\mathrm{i}\Delta}^{+\infty+\mathrm{i}\Delta} \frac{d\omega}{\pi}\frac{\omega}{\omega + \mathrm{i}k(\omega)c}E_i(\omega)\mathrm{e}^{-\mathrm{i}\omega t - k(\omega)z}, \quad z > 0. \quad (6)$$

For the following quantity included in expressions (5) and (6)

$$k(\omega) = \sqrt{-\frac{\omega^2}{c^2}\varepsilon_{tr}(\omega)} \quad (7)$$

for computing a square root, choose the branch $\mathrm{Re}[k(\omega) > 0]$, which provides damping of the plasma-penetrating field at $z \to +\infty$.

2. Aperiodic instability of the resultant multi-photon plasma ionization

Plasma generated via multi-photon ionization is instable with respect to evolution of aperiodic electromagnetic instability. Based on the findings from [27], we give the key data on this instable mode necessary for further

calculation of the structure of the electromagnetic field interacting with the given photoionized plasma. This instability is caused, firstly, by a non-equilibrium peak-shaped photoelectron energy distribution. Secondly, a non-monotonic dependence of effective frequency $\nu(v)$ of elastic photoelectron collisions with neutral atoms of inert gases on photoelectron velocity v, which is characterized by clearly pronounced minimum in the energy domain ~ 1 eV and corresponds to the Ramsauer–Townsend effect [32–34], plays an important role.

Explicit form of frequency $\nu(v) = Nv\sigma(v)$ takes into account the dependence of the transport cross-section of elastic photoelectron scattering $\sigma(v)$ by neutral atoms with concentration N on the photoelectron velocity. For Xe gas, this dependence σ was experimentally found in [36,37].

Following [27], we limit ourselves to the „cold" plasma model where photoelectron velocity distribution is approximated by $f_0(v) = \left(n/4\pi v_0^2\right)\,\delta(v - v_0)$, where $\delta(x)$ — is the Dirac delta function, v_0 is the photoelectron velocity in the energy peak. Such simple model makes it possible to use a closed-form solution almost completely. In this case, the transverse permittivity (4) takes an algebraic form

$$\varepsilon_{tr}(\omega) = 1 - \frac{\omega_L^2}{\omega\,(\omega + \mathrm{i}\,\nu_0)}\left(1 - \frac{\beta}{3}\frac{\mathrm{i}\,\nu_0}{\omega + \mathrm{i}\,\nu_0}\right). \qquad (8)$$

Here, $\nu_0 \equiv \nu(v_0)$, and the velocity-dependent quantity $\beta \equiv \beta(v_0) = d\ln[\nu(v)]/d\,\ln v|_{v=v_0}$ allows for considering the significant influence (defined by the Ramsauer–Townsend effect) of the dependence of photoelectron collision frequency on photoelectron velocity on the plasma mode properties.

$\beta(v)$ was explicitly derived and investigated using an approach proposed in [27], which is based on detailed experimental data reported in [37] in a wide range of photoelectron energies corresponding to the multi-photon condition where, in particular, evolution of the given aperiodic instability is possible. In this range, $\beta(v)$ has highly non-monotonic behavior driven by $\sigma(v)$, which distinguish our approach from works [22,38], which use a simple power interpolation for simulation of $\sigma(v)$.

We give typical effective frequencies of photoelectron collisions with neutral atoms ν_0 and with each other $\nu_{ee} = 4\pi e^4 n\Lambda/m^2 v_0^3$, where $\Lambda = \ln[2\pi n v_0^3/\omega_L^3]$ — is the Coulomb logarithm, defining the boundaries of the time range $\nu_0^{-1} < t \ll \nu_{ee}^{-1}$, during which a weakly varying non-equilibrium isotropic photoelectron distribution can exist in the form of a clearly pronounced monoenergetic peak, in particular, simulated by the δ-function. It is the time range where the test radiation amplification described below is possible. For conditions implemented in experimental study [7] where ionization of Xe atoms was performed through absorption of 11 Nd:YAG laser photons, photoelectron energy was equal to $mv_0^2/2 = 0.72$ eV. Cross-section of photoelectron scattering by neutral atoms is $\sigma = 0.4 \cdot 10^{-16}\,\mathrm{cm}^2$ and close to its lowest value [37], thus minimizing the corresponding collision frequency ν_0. With

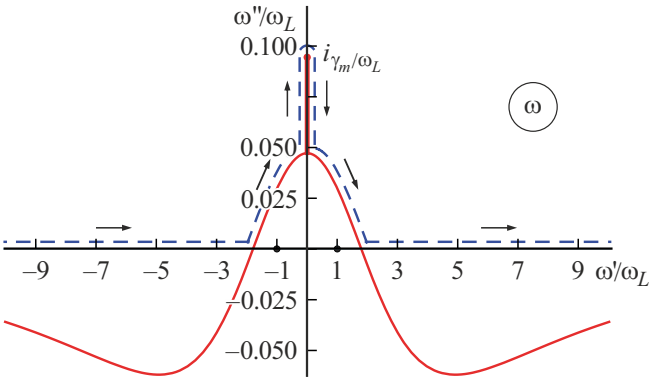

Figure 1. Frequency of aperiodically instable eigen mode of photoionized plasma (red solid line) in the plane of the complex frequency $\omega = \omega' + \mathrm{i}\,\omega''$ assigned to the electron plasma frequency ω_L. The curve is built for the Xe gas plasma with the neutral atom density $N \approx 2.5 \cdot 10^{19}\,\mathrm{cm}^{-3}$ generated via absorption by atoms of three KrF laser photons, when the photoelectron energy is 2.87 eV, and the degree of ionization is 10^{-5}. The dashed blue line shows the transformed integration path in expressions (5), (6).

near-atmospheric gas pressure, when atom concentration $N \approx 2.5 \cdot 10^{19}\,\mathrm{cm}^{-3}$, with the degree of ionization taken as 10^{-6}, we get the following estimates: $\nu_0 \approx 0.5 \cdot 10^{11}\,\mathrm{s}^{-1}$ and $\nu_{ee} \approx 1 \cdot 10^9\,\mathrm{s}^{-1}$. In this cases, the electron Langmuir frequency $\omega_L \approx 2.8 \cdot 10^{11}\,\mathrm{s}^{-1}$. In another case, when Xe atoms are ionized by $K = 3$ KrF laser photons, the photoelectron energy is much higher 2.87 eV [21] and the scattering cross-section grows to $\sigma = 1.5 \cdot 10^{-15}\,\mathrm{cm}^2$ [37], leading to even more significant difference of the above-mentioned collision frequencies. Taking the degree of ionization in this case as 10^{-5}, we have $\nu_0 \approx 3.8 \cdot 10^{12}\,\mathrm{s}^{-1}$ and $\nu_{ee} \approx 1.5 \cdot 10^9\,\mathrm{s}^{-1}$, $\omega_L \approx 8.9 \cdot 10^{11}\,\mathrm{s}^{-1}$. Thus for plasmas with the parameters selected above, the existence range of non-equilibrium isotropic photoelectron distribution in the form of a narrow monoenergetic peak is quite wide.

Taking the spatial field structure in plasma as e^{ikz}, where k is the wavenumber, a dispersion equation for eigen modes of the given photoionized plasma can be derived from (3). Detailed investigation of dispersion laws for these modes in the entire range of wavenumbers, of mode dissipative properties, and of the plasma parameter effect on the modes, in particular, photoelectron energy and density, was performed in [27]. In Figure 1 in the plane of complex frequency $\omega = \omega' + \mathrm{i}\,\omega''$ assigned to ω_L, a solid curve illustrates common properties of the complex frequency of the aperiodically instable mode using the case of Xe plasma with atmospheric density, which is generated via absorption by atoms of three KrF laser photons, when the photoelectron energy is 2.87 eV, and the degree of ionization is 10^{-5}. Along this curve, the wavenumber varies from $-\infty$ on the left at $\omega' \to -\infty$ to $+\infty$ on the right at $\omega' \to +\infty$. In the range of relatively low wavenumbers $0.05\,\omega_L/c \le |k| \le 1.86\,\omega_L/c$, the specified mode is an unstable electromagnetic wave,

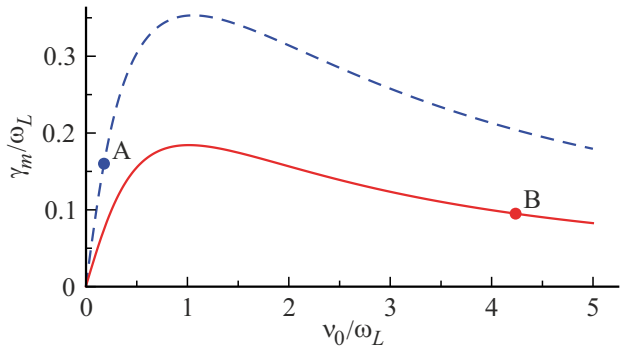

Figure 2. Dependence of the dimensionless maximum increment of aperiodic instability γ_m/ω_L on the dimensionless collision frequency ν_0/ω_L for Xe plasmas with the photoelectron energy: 0.72 eV (dashed curve) and 2.87 eV (solid curve. Points drawn on the curves correspond to two different photoionized plasmas with neutral atom density $N \approx 2.5 \cdot 10^{19}\,\mathrm{cm}^{-3}$ and degree of ionization 10^{-6} (**A**) and 10^{-5} (**B**), respectively, as described in Section 2.

whose real frequency decreases as $|k|$ decreases. In the extremely low wavenumber domain (long-wavelength limit), the mode becomes aperiodically instable (vertical segment of the curve along the imaginary axis in Figure 1). Maximum increment of this mode $\omega'' = \gamma_m < \omega_L$ is achieved at $k = 0$ and can be calculated from the cubic equation

$$\varepsilon_{tr}(\mathrm{i}\gamma_m) = 0. \tag{9}$$

Following [27], an exact closed-form solution to this equation is written as

$$\gamma_m = \omega_L \cdot \Gamma\left(\frac{\nu_0}{\omega_L}, \beta\right), \tag{10}$$

where

$$\Gamma(\xi,\beta) = a(\xi,\beta) + b(\xi,\beta), \tag{11}$$

$$a(\xi,\beta) = \left(\frac{\xi^3}{27} + \xi\frac{\beta-1}{6} + \frac{1}{3}\sqrt{\xi^4\frac{\beta}{9} + \xi^2\left[\left(\frac{\beta-1}{2}\right)^2 - \frac{1}{3}\right] + \frac{1}{3}}\right)^{\frac{1}{3}},$$

$$b(\xi,\beta) = \frac{\xi^2 - 3}{9\,a(\xi,\beta)}.$$

Figure 2 shows a curve of function (11), describing the dependence of the dimensionless maximum increment of aperiodic instability γ_m/ω_L on the dimensionless collision frequency ν_0/ω_L for two different photoionized plasmas Xe described in Section 2. The dashed line corresponds to the plasma with a photoelectron energy of 0.72 eV, the solid curve corresponds to $mv_0^2/2 = 2.87$ eV, respectively. Figure 2 demonstrates that function (10) has an non-sharp maximum for collision frequencies close to the electron Langmuir frequency. Asymptotic behavior of γ_m, according to (10), (11), in weak and strong collisional limits is described by simple expressions

$$\gamma_m \approx \left(\frac{\beta}{3} - 1\right) \cdot \begin{cases} \nu_0, & \nu_0 \ll \omega_L, \\ \omega_L^2/\nu_0, & \nu_0 \gg \omega_L. \end{cases} \tag{12}$$

Thus the aperiodic instability is possible provided that $\beta/3 > 1$ is fulfilled. This inequality is implemented in the given Xe plasma in a relatively wide range of photoelectron energies $0.65\,\mathrm{eV} < mv_0^2/2 < 4.1\,\mathrm{eV}$ [27]. Maximum $\beta/3 - 1 \approx 1.9$ is achieved for 0.95 eV. For conditions described in [7], when $mv_0^2/2 = 0.72$ eV, $\beta/3 - 1 \approx 1.0$ [27]. For the atmospheric gas density and degree of ionization 10^{-6} chosen above, in this case we get $\nu_0/\omega_L \approx 0.18$, and the relative maximum increment $\gamma_m/\omega_L = 0.16$, which corresponds to the „weak collisional", limit (upper line in (12)). In Figure 2, point **A** corresponds to this case. Absolute increment of aperiodic instability is $\gamma_m = 0.45 \cdot 10^{11}\mathrm{s}^{-1} \approx \nu_0$. In plasma generated via ionization by three radiation photons [21] where photoelectron energy is 2.87 eV, $\beta/3 - 1 \approx 0.5$ [27]. In such plasma generated from atmospheric-density gas with a degree of ionization of 10^{-5}, the „strong collisional" limit (lower line in (12)) $\nu_0/\omega_L \approx 4.2$ is implemented, and the relative maximum increment $\gamma_m/\omega_L = 0.095$ (point **B** in Figure 2). However, the absolute increment in this case appears to be higher than that in the previous case $\gamma_m = 0.85 \cdot 10^{11}$ with^{-1}. Note that according to [27], the maximum increment in Xe plasma can be $\gamma_m \approx 0.56\omega_L$ at $mv_0^2/2 \approx 0.89$ eV and $\nu_0 \approx 1.15\omega_L$. Thus, typical highest increments of aperiodic instability γ_m of the given photoionized plasmas appear to be comparable with (but not exceeding) the electron Langmuir frequency and correspond to the terahertz frequency range.

In a small neighborhood of $k = 0$, frequency of the given aperiodically instable eigen mode is merely imaginary and can be represented as

$$\omega'' = \gamma_m - \frac{k^2c^2}{\alpha^2\gamma_m}, \tag{13}$$

where taking into account equation (9)

$$\alpha^2 = \omega\left.\frac{\partial\varepsilon_{tr}(\omega)}{\partial\omega}\right|_{\omega=\mathrm{i}\gamma_m} \equiv \frac{(2\gamma_m+\nu_0)^2 + \omega_L^2 - \gamma_m^2}{(\gamma_m+\nu_0)^2} > 0. \tag{14}$$

Numerical values of α (14) for two different cases of photoionized plasma described in the beginning of Section 2 are 8.4 and 1.05, respectively. Closed-form expressions (10) and (11) for the maximum increment of aperiodically instable mode γ_m and expressions (13) and (14) for the increment expansion near γ_m will be used in the next section to describe the time-rising response of photoionized plasma to the incident radiation action (1).

3. Incident wave field amplification

In Section 3, we find the response of the plasma generated in advance in the multi-photon ionization conditions to

the action of an external electromagnetic pulse (1). Using integral expressions for reflected wave field (5) and plasma-penetrating field (6) derived in Section 1, we establish the spatiotemporal radiation structure established. Expressions (5) and (6) are used to explore the action of various pulse waveforms on the plasma. An incident monochromatic wave field written as

$$E_i\,(t - z/c) = E_L \cdot \sin\left[\omega_0\,(t - z/c)\right], \qquad (15)$$

where E_L is the amplitude, ω_0 is the test radiation frequency, is discussed below, and the Laplace image of such filed is written as $E_i\,(\omega) = E_L \cdot \omega_0/(\omega_0^2 - \omega^2)$. We rely on the results obtained in [27] for both closed-form and numerical calculations of the dispersion law for the instable mode described in the previous section. We deform the standard integration path (5) and (6) into a path enveloping the given mode frequency curve in the plane of complex variable $\omega = \omega' + \mathrm{i}\,\omega''$ and shown by a dashed line in Figure 1. Then, expressions for field in vacuum and plasma can be broken down into a sum of two contributions

$$E_r(t + z/c) = E_r^{(\omega)}(t + z/c) + E_r^{(\gamma)}(t + z/c), \quad z < 0,$$

$$E(z,t) = E^{(\omega)}(z,t) + E^{(\gamma)}(z,t), \quad z > 0. \qquad (16)$$

Contributions with index (ω) are formed through integration by the path segments along the real axis at $\omega'' = 0$ and describe time-rising harmonic fields with frequency close to the incident wave frequency ω_0. On the contrary, summands with index (γ) correspond to the integration path segments lying above the real axis $\omega'' > 0$. It is these contributions that describe the time-rising fields related to the evolution of aperiodic instability in plasma. It is obvious that the main contribution to integrals (5) and (6), defining the time-rising plasma response, is made by the values of integration variable along the positive segment of the imaginary axis near the maximum increment γ_m. Relying on expansion (13) applicable in the small neighborhood $\omega = \mathrm{i}\,\omega'' \approx \mathrm{i}\gamma_m$, the following approximate expression for function (7) can be written as:

$$k(\mathrm{i}\omega'') \approx \mp\,\mathrm{i}\,\alpha\,\frac{\gamma_m}{c}\sqrt{1 - \frac{\omega''}{\gamma_m}},$$

$$0 < \gamma_m - \omega'' \ll \gamma_m, \qquad (17)$$

where the upper and lower signs correspond to the left-hand and right-hand vertical segments of the integration path along the imaginary axis. Then, at large times $t \gg \gamma_m^{-1}$, using the saddle-point method [41], expressions (5) and (6) give the following asymptotic expressions for time-rising parts of the reflected wave field

$$E_r^{(\gamma)}\left(t + \frac{z}{c}\right) \approx -\frac{\alpha}{\sqrt{\pi}}\,\gamma_m E_i\,(\mathrm{i}\gamma_m)\,\frac{\mathrm{e}^{\gamma_m\,(t+z/c)}}{\left[\gamma_m\,(t + z/c)\right]^{3/2}}, \quad z < 0. \qquad (18)$$

and plasma-penetrating field both near the plasma boundary and decreasing to the depth

$$E^{(\gamma)}\,(z,t) \approx -\frac{\alpha}{\sqrt{\pi}}\,\gamma_m E_i\,(\mathrm{i}\gamma_m)$$

$$\times \begin{cases} \left(1 + \dfrac{\gamma_m z}{c}\right)\dfrac{\mathrm{e}^{\gamma_m t}}{(\gamma_m t)^{3/2}}, & 0 < z \ll \dfrac{2}{\alpha}\,c\,\sqrt{\dfrac{t}{\gamma_m}}, \\ \left(\dfrac{\alpha^2}{2} + \dfrac{ct}{z}\right)^{-1}\dfrac{\mathrm{e}^{\gamma_m\left(t - \frac{\alpha^2}{4}\frac{z^2}{c^2 t}\right)}}{\sqrt{\gamma_m t}}, & \dfrac{2}{\alpha}\,c\,\sqrt{\dfrac{t}{\gamma_m}} \ll z < ct. \end{cases} \qquad (19)$$

In the case of explicit incident field (15), $\gamma_m E_i\,(\mathrm{i}\gamma_m) = E_L\,\gamma_m\omega_0/(\gamma_m^2 + \omega_0^2)$. From this it follows that radiation with frequency close to the maximum increment of aperiodically instable mode of photoionized plasma $\omega_0 \sim \gamma_m$ will be enhanced most effectively. Expressions (18) and (19) demonstrate that the time rise of the most effectively amplified response of non-equilibrium plasma is defined by the maximum increment of the aperiodic instability γ_m evolving in plasma, while the amplitude is also defined by the external radiation strength and frequency.

Figure 3 shows a spatial structure of the electric field $E(z,t)$ in plasma $z > 0$ and of the full field $E_i(t - z/c) + E_r(t + z/c)$ upstream of plasma $z < 0$ for different times corresponding to $\gamma_m t = 2.5$ — (Figure 3, *a*), 5 — (Figure 3, *b*), 7.5 — (Figure 3, *c*) and 10 — (Figure 3, *d*), respectively, assigned to the incident wave amplitude E_L depending on the dimensionless coordinate $\omega_L z/c$. The same plasma parameters were chosen as in Figure 1. Radiation frequency is $\omega_0 \approx 0.12\,\omega_L \approx 1.1 \cdot 10^{11}\,\mathrm{s}^{-1}$ and, according to the estimates from the previous section, corresponds to the lower part of the THz frequency range. At the same time, $\omega_0 \approx 1.26\gamma_m$, which is close to the optimum amplitude amplification conditions. Figure 3 demonstrates that the field penetrates the plasma to the depth $z < ct$ and is reflected from the plasma, rising exponentially quickly with time. Amplification of the plasma response strength can reach several orders of magnitude compared with the incident wave amplitude. The insert in Figure 3, *c* shows the incident wave field $E_i(t - z/c)$ (solid red line) and the time-rising reflected wave field $E_r(t + z/c)$ (dashed blue line) separately from each other. Note that in the long-wavelength approximation used in kinetic equation (2) without considering the spatial dispersion of plasma permittivity (4), description of fields (15) near the field propagation edges at $z \approx \pm ct$ is not accurate. However, this is irrelevant when describing the time-rising portion of plasma response. For photoionized plasma with parameters used for drawing the curves in Figure 3, normal skin effect conditions are implemented where the skin layer depth is calculated using expression [35] $\delta = (c/\omega_L)\sqrt{2\nu_0/(\beta/3 - 1)|\omega|}$. In the instability conditions $|\omega| = \gamma_m$ and for the given plasma, the lower line of limiting expression (12) is applicable. Then $\delta = \sqrt{2}\,(\beta/3 - 1)^{-1}(c\,\nu_0/\omega_L^2) = \sqrt{2}\,c/\gamma_m \approx 0.5\,\mathrm{cm}$. The way in which these figures demonstrate the maximum

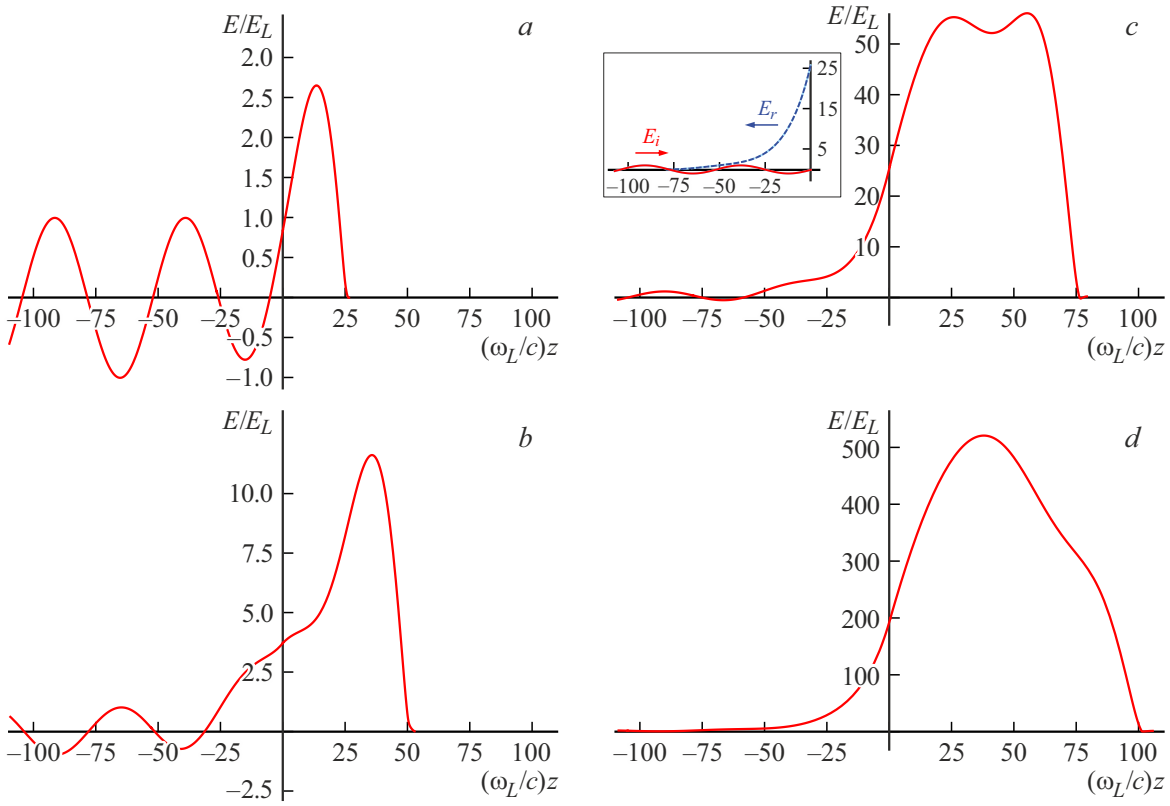

Figure 3. Spatial structure of electric field strength $E(z,t)$ in plasma $z > 0$ and full field strength $E_i(t - z/c) + E_r(t + z/c)$ upstream of plasma $z < 0$ assigned to the incident wave amplitude E_L as the dimensionless coordinate function $\omega_L z/c$. The curves were plotted in different times, when $\gamma_m t = 2.5$ — (a), 5 — (b), 7.5 — (c) and 10 — (d). Inset in Figure (c) illustrates the incident wave field $E_i(t - z/c)$ (solid red line) and the time-rising reflected wave field $E_r(t + z/c)$ (dashed blue line) separately from each other. The same plasma parameters as in Figure 1 were chosen. Radiation frequency is $\omega_0 \approx 0.12\,\omega_L$.

growth of the amplified field strength within the plasma is implemented on spatial scales of the order of several skin layer depth and is defined by values of the order of a centimeter. Note that our relatively simple closed-form solution is performed in the linear approximation both in the field amplitude (1) and at the linear stage of aperiodic instability evolution. Therefore, the obtained quantitative results are applicable at times lower than the initial non-equilibrium photoelectron distribution variation time and nonlinear instability saturation time, which is easily implemented for test fields with a small intensity compared with the ionizing radiation.

Summarizing Section 3, focus is made on justifying the applicability of the employed homogeneous plasma half-space model with stepwise electron density variation at the boundary in studying the features of interaction between the test radiation and photoionized gas plasma. Such plasma is generated under the ionizing action of the intense laser pulse with a duration of several tens of femtoseconds and is localized in the pulse focusing area, and the photoelectron density decreases from the focusing center to outside, which requires the employed approximation to be discussed. Paper [35] is devoted to investigating the effect of spatial scale of plasma boundary smearing on the modes of plasma exposure to the test electromagnetic radiation, in particular, to establishing the conditions of applicability of the stepwise photoelectron density variation assumption. It is reported in [35] that, if the variable-density boundary layer thickness is smaller than the skin layer depth, then the consideration of plasma boundary smearing doesn't provide any significant corrections compared with the sharp boundary model. For photoionized plasma described in [21] with parameters used for drawing Figures 1−3, normal skin effect conditions are implemented where the skin layer depth is $\delta \approx 0.5$ cm. Typical focal spot sizes of modern femtosecond lasers may be from several units to several hundreds of micrometers, and when gases with near-atmospheric density are exposed to such lasers, laser plasma is generated, at whose boundary electron density grows on scale of several micrometers, which is much smaller than δ, thus making the sharp plasma model justified in [35] applicable. Note that boundary smearing due to plasma expansion in electroneutrality conditions is defined by cold ions and has a rate compared with ion-sound velocity $\sim \sqrt{m/M}\,v_0$ (M is the ion mass), and doesn't exceed several electron Debye radii [42] $v_0/\omega_L \approx 3.3 \cdot 10^{-3} c/\omega_L \approx 10^{-4}$ cm in the non-equilibrium narrow-peak photoelectron energy distribution lifetime range and also doesn't prevent from using the sharp

plasma boundary model at non-equilibrium photoelectron distribution lifetimes.

Sizes of the generated plasma domain along the ionizing laser pulse distribution direction in gas are equal to several tens of centimeters [20,22,25], while the effective spatial zone of the test THz radiation amplification for the plasma described in Section 3 is concentrated in a much smaller domain whose sizes are of the order of several skin layer depths, i.e. of a centimeter. Opportunity to achieve a final closed-form solution result is one of the key advantages of the chosen simple one-dimensional plasma description model without considering transverse dimensions of the plasma domain.

Such approach is justified by the dominant role (as was identified during the study) of long-wavelength eigen instable aperiodic modes in the radiation amplification.

Consecutive consideration of transverse plasma dimensions and their impact on the radiation amplification efficiency is the aim of our further investigation.

Conclusion

Response of the non-equilibrium collisional weakly ionized semiconfined plasma pre-generated through multiphoton ionization of inert gas atoms by a short laser pulse to the action of external electromagnetic pulse was investigated in the linear approximation.

Investigation was performed on the basis of a consistent kinetic description of photoelectron dynamics and Maxwell's equations for fields using the Laplace time transform, providing consecutive description of instability evolution in the semiconfined plasma within the initial problem. General integral expressions for fields were derived, admitting different waveforms of pulse applied to the plasma and offering detailed description of the spatial radiation structure in the entire space and of radiation time evolution at the linear instability evolution stage. Due to non-equilibrium photoelectron energy distribution and features of photoelectron scattering by neutral atoms associated with the Ramsauer–Townsend effect, aperiodic electromagnetic instability may develop in such plasma. It is shown that as a result of interaction between such instable plasma and harmonic plane wave, besides a response at the external field frequency, there is a dominant anharmonic time amplification of both penetrating and reflected fields in a broad frequency band concentrated at the maximum increment of aperiodic photoionized plasma instability.

Typical amplification coefficients may reach several orders of magnitude. For ionized gas densities near the atmospheric density, the typical increment falls into the THz range. This indicates a new opportunity of using the abovementioned photoionized plasma response mechanism for electromagnetic radiation amplification or generation in the terahertz frequency range.

Conflict of interest

The author declares no conflict of interest.

References

[1] N.B. Delone, V.P. Krainov. JOSA B, **8**, 1207 (1991). DOI: 10.1364/JOSAB.8.001207
[2] S.J. McNaught, J.P. Knauer, D.D. Meyerhofer. Phys. Rev. Lett., **78**, 626 (1997). DOI: 10.1103/PhysRevLett.78.626
[3] W.P. Leemans, C.E. Clayton, W.B. Mori, K.A. Marsh, P.K. Kaw, A. Dyson, C. Joshi, J.M. Wallace. Phys. Rev. A, **46**, 1091 (1992). DOI: 10.1103/PhysRevA.46.1091
[4] V.D. Mur, S.V. Popruzhenko, V.S. Popov. JETP, **92**, 777 (2001). DOI: 10.1134/1.1378169
[5] C.K. Huang, C.J Zhang, K.A. Marsh, C.E. Clayton, C. Joshi. Plasma Phys. Control. Fusion, **62**, 024011 (2020). DOI: 10.1088/1361-6587/ab61df
[6] P. Agostini, F. Fabre, G. Mainfray, G. Petite, N.K. Rahman. Phys. Rev. Lett., **47**, 1127 (1979). DOI: 10.1103/PhysRevLett.42.1127
[7] G. Petite, P. Agostini, F. Yergeau. JOSA B, **4**, 765 (1987).
[8] H.G. Muller, H.B. van Linden van den Heuvell, P. Agostini, G. Petite, A. Antonetti, M. Franco, A. Migus. Phys. Rev. Lett., **60**, 565 (1988). DOI: 10.1103/PhysRevLett.60.565
[9] F. Fabre, P. Agostini, G. Petite, M. Clement. J. Phys. B: Atom. Mol. Phys., **14**, L677 (1981). DOI: 10.1088/0022-3700/14/21/007
[10] Y. Gontier, N.K. Rahman, M. Trahin. EPL, **5**, 595 (1988). DOI: 10.1209/0295-5075/5/7/004
[11] T. Marchenko, H.G. Muller, K.J. Schafer, M.J.J. Vrakking. J. Phys. B: At. Mol. Opt. Phys., **43**, 185001 (2010). DOI: 10.1088/0953-4075/43/18/185001
[12] M. Li, Y. Liu, H. Liu, Y. Yang, J. Yuan, X. Liu, Y. Deng, C. Wu, Q. Gong. Phys. Rev. A, **85**, 013414 (2012). DOI: 10.1103/PhysRevA.85.013414
[13] L. Zhang, Z. Miao, W. Zheng, X. Zhong, C. Wu. Chem. Phys., **523**, 52 (2019). DOI: /10.1016/j.chemphys.2019.04.005
[14] A.V. Timofeev. Plasma Phys. Rep., **38**, 79 (2012). DOI: 10.1134/S1063780X11120099
[15] K.Y. Vagin, S.A. Uryupin. JETP, **111**, 670 (2010). DOI: 10.1134/S1063776110100195
[16] K.Y. Vagin, S.A. Uryupin. Plasma Phys. Rep., **39**, 674 (2013). DOI: 10.1134/S1063780X13080060
[17] K.Y. Vagin, S.A. Uryupin. Plasma Phys. Rep., **40**, 393 (2014). DOI: 10.1134/S1063780X14040096
[18] K.Y. Vagin, S.A. Uryupin. Plasma Phys. Rep., **41**, 744 (2015). DOI: 10.1134/S1063780X15080103
[19] Z. Donko, N. Dyatko. Eur. Phys. J. D, **70**, 135 (2016). DOI: /10.1140/epjd/e2016-60726-4
[20] A.V. Bogatskaya, N.E. Gnezdovskaia, E.A. Volkova, A.M. Popov. Plasma Sources Sci. Technol., **29**, 105016 (2020). DOI: 10.1088/1361-6595/aba110
[21] A.V. Bogatskaya, A.M. Popov. JETP Lett., **97**, 388 (2013). DOI: 10.1134/S0021364013070035
[22] A.V. Bogatskaya, A.M. Popov. Laser Phys. Lett., **16** (6), 066008 (2019). DOI:10.1088/1612-202X/ab183d
[23] K.Yu. Vagin, S.A. Uryupin. Plasma Sources Sci. Technol., **29**, 035005 (2020). DOI: 10.1088/1361-6595/ab5e28

[24] K.Yu. Vagin, S.A. Uryupin. Phys. Plasmas, **27**, 112110 (2020). DOI: 10.1063/5.0023518
[25] A.V. Bogatskaya, E.A. Volkova, A.M. Popov. Phys. Rev. E, **104**, 025202 (2021). DOI: 10.1103/PhysRevE.104.025202
[26] A.V. Bogatskaya, E.A. Volkova, A.M. Popov. J. Opt. Society America B, **39** (1), 299 (2022). DOI: 10.1364/JOSAB.435710.
[27] K.Y. Vagin, S.A. Uryupin. Plasma Phys. Reports, **49** (9), 1104 (2023). DOI: 10.1134/S1063780X23600998
[28] V.A. Kostin, I.D. Laryushin, A.A. Silaev, and N.V. Vvedenskii. Phys. Rev. Lett., **117** (3), 035003 (2016). DOI: 10.1103/PhysRevLett.117.035003
[29] A.A. Silaev, A.A. Romanov, N.V. Vvedenskii. Opt. Lett., **45** (16), 4527 (2020). DOI.org/10.1364/OL.394979
[30] M. Gao, X. Xu, J. Lou, R. Wang, Z. Zhang, Z. Wen, C. Chang, Y. Huang. Phys. Rev. Res., **5** (2), 023091 (2023). DOI: 10.1103/PhysRevResearch.5.023091
[31] H.A. Lorentz. Arch. Neerl. **10**, 336 (1905). (see also *Lorentz H.A.* Collected Papers (Martinus Nijhoff, The Hague, 1936), Vol. III.)
[32] J.S. Townsend, V.A. Bailey. The London, Edinburgh, and Dublin Philosophical Magazine and Journal of Science, **42**, 873 (1921).
[33] C. Ramsauer. Annalen der Physik, **369**, 513 (1921).
[34] R.B. Brode. Reviews of Modern Physics, **5**, 257 (1933).
[35] K.Y. Vagin, T.V. Mamontova, S.A. Uryupin. Phys. Rev. E, **104** (4), 045203 (2021). DOI:10.1103/PhysRevE.104.045203
[36] M. Hayashi. J. Phys. D: Appl. Phys., **16**, 581 (1983). DOI: 0.1088/0022-3727/16/4/018
[37] M. Hayashi. *Bibliography of electron and photon cross sections with atoms and molecules published in the 20th century* (Xenon: Tech. Rep.: : National Inst. for Fusion Science 2003.)
[38] A.V. Bogatskaya, H. Bin, A.M. Popov, I.V. Smetanin. Phys. Plasmas, **23** (9), 023091 (2016).
[39] A.B. Mikhailovskii. *Teoriay plazmennykh neustochivostei. T.1: Neustoichivosti odnorodnoy plazmy* (Atomizdat, M., 1970), 294 s. (in Russian)
[40] B.M. Smirnov. *Physics of ionized gases* (John Wiley & Sons, NY., 2001)
[41] F.W.J. Olver. *Introduction to Asymptotics and Special Functions* (Academic Press, NY. and London, 1974), 297 p.
[42] J.E. Allen, M. Perego. Phys. Plasmas, **21** (3), 045203 (2014). DOI: 10.1063/1.4870084

Translated by E.Ilyinskaya